Recent Res. Devel. Atmos. Sci., 1(2001):15-37 ISBN : 81 - 7736 - 059 - 0

Obliquity modulation of the incoming solar radiation

Han-Shou Liu
NASA Goddard Space Flight Center, Greenbelt, MD 20771, U.S.A.

International Gold Medal Award

2001

ABSTRACT

Based on a basic principle of orbital resonance, we have identified a huge deficit of solar radiation induced by the combined amplitude and frequency modulation of the Earth's obliquity as possibly the causal mechanism for ice age glaciation. Including this modulation effect on solar radiation, we have performed model simulations of climate change for the past 2 million years. Simulation results show that: (1) For the past 1 million years, temperature fluctuation cycles were dominated by a 100-Kyr period due to amplitude-frequency resonance effect of the obliquity. (2) From 2 to 1 million years ago, the amplitude-frequency interactions of the obliquity were so weak that they were not able to stimulate a resonance effect on solar radiation. (3) Amplitude and frequency modulation analysis on solar radiation provides a series of resonance in the incoming

solar radiation which may shift the glaciation cycles from 41-Kyr to 100-Kyr about 0.9 million years ago. These results are in good agreement with the marine and continental paleoclimate records. Thus, the proposed climate response to the combined amplitude and frequency modulation of the Earth's obliquity may be the key to understanding the glaciation puzzles in paleoclimatology.

1. INTRODUCTION

Incoming solar radiation, generally called "insolation," is a key factor in climate change studies. Deviations of the incoming solar radiation depend upon astronomical parameters which characterize the orbit of the Earth around the Sun and the Earth's axis of rotation. An equation for the insolation deviations was formulated and solved by Milankovitch [1] and Vernekar [2] using numerical procedure. In the conventional insolation theory for climate change, the Milankovitch insolation equation is considered as an external forcing function in climate models [3]. The periodicities of the Milankovitch insolation cycles always depend upon three orbital parameters: (1) orbital eccentricity e for the 100-Kyr cycle, (2) obliquity ε for the 41-Kyr cycle, and (3) precession index $e \sin \omega$ for the 23-or 19-Kyr cycle (ω is the argument of perihelion).

For several decades, geophysicists have been trying to develop physical mechanisms in which the 100-Kyr cycles in the ellipticity of the Earth's orbit around the Sun shift the pattern of insolation, triggering the growth and decay of great ice sheets in the high latitudes of the Northern Hemisphere. This effort has encountered great difficulty: The 100-Kyr orbital eccentricity cycle is too small in amplitude and too late in phase [3, 4] to produce the 100-Kyr glaciation cycle during the last 1 million years. This is one of the most perlexing and enduring puzzles in paleoclimatology.

The second puzzle is how to explain the ice sheet cycles in the Northern Hemisphere from 1 million to 2 million years ago when the global ice volume and deep sea temperature varied at an almost metronomic 41-Kyr period of the Earth's obliquity. Thirdly, we still do not understand why the 100-Kyr ice age cycle become dominant about 0.9 million years ago. Numerous hypotheses and models have been proposed to explain these glaciation puzzles. Proposed explanations for these puzzles have invoked: (1) stochastic resonance of eccentricity forcing [5], (2) internal oscillations of the climate system near the 100-Kyr period that can get phase-locked to external (eccentricity) forcing [6], (3) high nonlinear response of climate system to weak forcing by the orbital eccentricity [3, 7-13], (4) variations in the inclination of the Earth's orbital motion [14-16] and (5) climate system with three steady states and a set of predefined rules for moving between them [17]. However, the physical mechanisms of the glaciation cycles are unknown.

From dynamics point of view, Liu [18,19] has shown that the 100-Kyr periodicity of the ice ages is not due to eccentricity at all, but to frequency variations in the obliquity, which is the tilt angle of the Earth's rotation axis from its orbital plane. Indeed, Rubincam [20,21] has obtained an analytical insolation equation which shows that neither the main pacemaker of the ice age e, nor Milankovitch precession index $e \sin \omega$ appear as terms in the equation, but obliquity ε does. Rubincam's analytical insolation equation is developed in terms of spherical harmonies. It is a convenient formula for computing insolation forcing when using

numerical climate models. In a series of papers [22-25], we have used numerical climate models to demonstrate that frequency modulation of the Earth's obliquity is responsible and accountable for major climate changes during the past 2 million years. For a physical mechanism to be considered appropriate and convincing, we have computed variations in the solar energy flux at the top of the atmosphere and identified that the insolation flux deficit is the physics behind the ice age glaciation.

We should emphasize that our interest in this study does not lie in the mathematical development of celestial mechanics and sophisticated climate modeling. Rather, we are concerned with the necessary, fundamental concepts in wave physics to understand the climate cycles as seen in oxygen isotopic $\delta^{18}0$ measurements from ocean sediment cores [26-29] and biogenic silica measurements from continental sediment cores in Lake Baikar [30].

Finally, we note that the obliquity modulation theory for climate change in this study is developed in order to relate the variations of the Earth's obliquity and its derived frequency to climate. However, changes in the solar constant due to natural evolution of the Sun as a star or related to sunspots will not be part of the theory. Different astronomical theories of paleoclimate, such as those of LeVerrier [31], Croll [32], Milankovitch [1], Vernekar [2] Berger and Loutre [33] and Rubincam [20,21], fall under such a definition.

2. OBLIQUITY VARIATIONS

Lunar and solar gravitational torques acting on the equatorial bulge of the Earth cause its spin axis to precess about the instantaneous orbital normal. The lunar and solar torques together produce a precession of the spin axis of the Earth at a rate of 50.38 arcsec yr^{-1} [34,35]. Once the present spin axis direction is known and orbital element histories are given, the obliquity history can be constructed by applying the methods developed by Brouwer and van Woerkom [36]. In this way the variations in the Earth's obliquity have been determined by [2]:

$$\begin{aligned}\varepsilon(t) = \varepsilon^{*} &- \sum_{i=1} c_i N_i \cos\left[(s_i + K)t + \delta_i + \alpha\right] \\ &- \sum_{i=1} c_{ii} N_i^2 \cos\left\{2\left[(s_i + K)t + \delta_i + \alpha\right]\right\} \\ &- \sum_{i=1}\sum_{j>1} C_{ij} N_i N_j \cos\left[(s_i + s_j + 2K)t + \delta_i + \delta_j + 2\alpha\right] \\ &- \sum_{i=1}\sum_{j>1} C_{ij} N_i N_j \cos\left[(s_i - s_j)t + \delta_i - \delta_j\right]\end{aligned} \quad (1)$$

In equation (1), t is the time and all constants were given in [2]. The variations in the obliquity were computed from equation (1) for the past 4000 Kyr with an interval of 1 Kyr by Vernekar [2]. His results showed that the obliquity of the Earth varied in the past 4000 Kyr only from 24.51^0 to 22.10^0, with an average period of 41 Kyr. The obliquity period of 41 Kyr has long been recognized as one for the Milankovitch glaciation cycles as seen in geological climate records. However, equation (1) represents a waveform with variable phase angles. Phase modulation may induce asymmetry of the obliquity cycles, permitting transient or time-dependent unstable climate features to be detected. This seems to be the pitfall in the Milankovitch theory for climate change by which we were led into interpretation difficulties of climate response to orbital forcing [3,37-40]. Probably the most important feature through which the orbital imprint may be unambiguously recognized in ancient geological records is the phase modulation of the obliquity component. Milankovitch theory is virtually valueless to detect this property in geological records. Actually, investigation of the phase

modulation effect of the obliquity on climate change requires complex representation of equation (1).

3. FREQUENCY MODULATION OF THE OBLIQUITY

In order to compute the frequency modulation of the obliquity, the complex representation of $\varepsilon(t)$ can be expressed by a complex waveform

$$\begin{aligned}\Delta\varepsilon(t) &= \varepsilon(t) - \varepsilon^{\circ} \\ &= \sum_{i=1} A_i \cos(\gamma_i t + \zeta_i) \\ &= r(t)\exp\left(\sqrt{-1}\theta(t)\right)\end{aligned} \qquad (2)$$

where A_i, r_i and ζ_i are the amplitude, mean frequency and phase for each component, respectively. The initial value of ε° is 23.230556° and t = 0 refers to AD 1950. All constants for i = 1,2,3,..... were given in [41,42]. The complex vector in equation (2) has a magnitude r(t) and angle $\theta(t)$ where r(t) is slowly varying and $\theta(t)$ varies rapidly. By setting the phase function

$$\theta(t) = \varpi_C t + \phi(t) \qquad (3)$$

where ϖ_C is the mean obliquity frequency and $\phi(t)$ is the phase angle of the obliquity, then

$$\begin{aligned}\hat{\Delta}\varepsilon(t) &= \Delta\varepsilon(t) \otimes \frac{1}{\pi t} = \frac{1}{\pi}\int_{-\infty}^{\infty} \frac{\Delta\varepsilon(\tau)}{t-\tau} d\tau \\ &= \frac{1}{\pi}\int_{-\infty}^{\infty} \frac{\Delta\varepsilon(t-\tau)}{\tau} d\tau \\ &= \sum_{i=1} A_i \sin(\gamma_i t + \zeta_i)\end{aligned} \qquad (4)$$

where $\hat{\Delta}\varepsilon(t)$ is the convolution of $\Delta\varepsilon(t)$ and $1/(\pi t)$. Therefore,

$$\phi(t) = \tan^{-1}\left[\frac{\sum_{i=1} A_i \sin(\gamma_i t + \zeta_i)}{\sum_{i=1} A_i \cos(\gamma_i t + \zeta_i)}\right] \qquad (5)$$

Liu, [18] has suggested that climate response to obliquity forcing may be determined by the frequency variation of the obliquity. In this case the instantaneous frequency $\varpi_i(t)$ of the phase-modulated obliquity is defined as the derivative of the phase:

$$\varpi_i(t) = \varpi_C + \frac{d\phi(t)}{dt} \qquad (6)$$

where $\varpi_c = 31.079137$ (arc·sec·yr^{-1}) and $d\phi/dt$ is the frequency deviation. Denoting

$$\Delta\varpi(t) = \frac{d\phi(t)}{dt} \qquad (7)$$

we may define a phase factor $\mu(t)$ as the ratio of the change rate of the phase function θ of the obliquity to the mean frequency of the obliquity. Thus

$$\begin{aligned}\mu(t) &= \frac{1}{\varpi_C}\frac{d\theta}{dt} = 1 + \frac{\Delta\varpi(t)}{\varpi_C} \\ &= \frac{1}{\varpi_C}\frac{d}{dt}\left\{\tan^{-1}\left[\frac{\sum_{i=1} A_i \sin(\gamma_i t + \zeta_i)}{\sum_{i=1} A_i \cos(\gamma_i t + \zeta_i)}\right]\right\}\end{aligned} \qquad (8)$$

which regulates climate model response to the incoming solar radiation.

The scientific basis of this study is the time series of the instantaneous frequency of the obliquity $\varpi_i(t)$ in equation (6). Variations of $\varpi_i(t)$ in time with their correspondence period variations are shown in Figure 1. Figure 1 shows that the period of the obliquity varied from about 37 Kyr to 44 Kyr for the past 1 million years. This lengthening/shortening

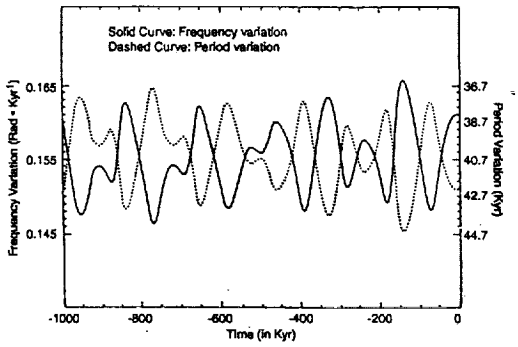

Figure 1. Frequency and period variations of the Earth's obliquity.

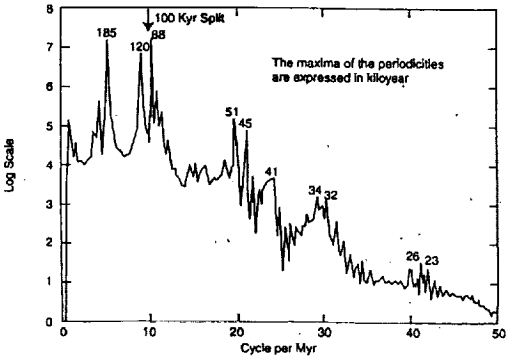

Figure 2. Spectral amplitude of the obliquity frequency variations.

effect of the obliquity period is closely associated with major paleoclimate events [18].

Also, Liu [18] has reported a prominent 100-Kyr peak in the spectrum of the ϖ_i (t) time series which may be related to the anomalous 100-Kyr peak in the $\delta^{18}O$ spectrum. An improved spectral amplitude of $\varpi_i(t)$ is shown in Figure 2. The physical interpretation of this spectrum may be made as follows: (1) it indicates that 185-Kyr climate cycles could be recorded in geological data, as suggested by Beaufort [40]; (2) the deep split of the 100-Kyr peak into two peaks at about 120-Kyr and 88-Kyr is of particular interest because the irregular ice age cycles varied from about 80 Kyr to 120 Kyr over the past 1 million years [19]; (3) the major peaks are seen at 100-Kyr and 185-Kyr, and the peaks at 41-Kyr and 26- to 23-Kyr have relatively low intensities with minor significance; and (4) the peak at 45-Kyr was recorded by the core data of V19-28 and V19-29 in the Pacific Ocean.

4. A TEST MODEL: FREQUENCY MODULATION EFFECT OF THE OBLIQUITY ON CLIMATE CHANGE

The hypothesis of frequency forcing of the obliquity for climate change is that glacial and interglacial intensities are related to the frequency variation of the obliquity. Ice ages started after the instantaneous frequency $\varpi_i(t)$ reached a low value. The physical concept was described by Liu [19], but its validity needs to be tested by simple but realistic climate models. A class of zero-dimensional energy balance models (EBM) for climate change with surface temperature T as the main variable was developed as one of the fundamental climate models [5, 43-46]. For a simplified version of EBM, the equation of the model is

$$c\frac{dT}{dt} = Q(t)[1-\alpha(T)] + E(T) \qquad (9)$$

where c is the thermal capacity of the Earth, Q(t) is the incoming solar radiation, $\alpha(T)$ is the globally averaged albedo, and $E(T)$ is the outgoing surface radiation. The formula for the albedo is [5].

$$\alpha(T) = d_1 - d_2 \tanh[d_3(T - T_*)] \qquad (10)$$

where d_1, d_2 and d_3 are constants. E (T) can be parameterized as a linear function of T through two empirical parameters A and B such that

$$E(T) = -(A + BT) \qquad (11)$$

Solar intensity Q(t) reaching the Earth may be modulated by the frequency variability of the obliquity [18,19], which is a function of the rate of change of the phase function θ as defined by equation (8). Thus

$$Q(t) = \mu(t)Q_o \qquad (12)$$

where Q_o is one quarter of the solar radiation intensity. The parameter $\mu(t)$ in equation (12) allows us to introduce explicit variations in the solar input. Accordingly, the equation of the EBM becomes

$$c\frac{dT}{dt} = \frac{1}{\varpi_c}\frac{d}{dt}\left[\tan^{-1}\left(\frac{\sum_{i=1} A_i \sin(\gamma_i t + \zeta_i)}{\sum_{i=1} A_i \cos(\gamma_i t + \zeta_i)}\right)\right] Q_o \cdot \left\{1 - d_1 + d_2 \tanh\left[d_3(T - T_s)\right]\right\} - A - BT \qquad (13)$$

The constants in equations (10) and (11) for albedo and the outgoing surface radiation are chosen to yield roughly the limits of the temperature range exhibited by the glacial-interglacial oscillations of the Pleistocene and, therefore, they could be interpreted as representing the glacial and interglacial states of the Earth's climate system. Using other parameterizations for the albedo and outgoing surface radiation [43, 44, 47], the model is able to produce slightly different results for comparison.

The estimates of the geophysical constants in equation(13) were given in [5] and all numerical values of orbital constants were given in [41, 42] for i = 1,2,3,.... . We have computed temperature T as a function of time from equation (13). With the above choices of the orbital constants and geophysical constants, we have obtained that the range of variations in T is about 11^0 C in paleoclimatic variations assuming a linear relationship between $\delta^{18}O$ and the surface temperature [48,49]. However, the 8^0C temperature change commonly inferred from core isotopic records [50-52] is relatively smaller than the recent estimates of the 15^0 C temperature change from central Greenland [53].

The time-dependent solution of equation (13) are derived from the lengthening/shortening of the obliquity cyclic period. In order to display the relationship between the temperature T and $\delta^{18}O$ variations, we have determined the time-dependent changes in the amplitude of the 100-Kyr frequency component in both the $T(t)$ and the $\delta^{18}O$ time series. The method of complex demodulation [54] allows us to make such a determination. Complex demodulation is carried out by first calculating the product of $T_{(t)}$ exp (i 2 π ft) where i is the square root of -1 and f is the 100-Kyr frequency at which we wish to determine the time-dependent changes in amplitude. Complex demodulation of the simulated temperature $T(t)$ and the complex demodulation of the $\delta^{18}O$ times series [55] are shown in Figure 3, indicating the general similarity between the results of simulaions and the observation data. Therefore the test model indicates that equation (13) can be used to generate a 100-Kyr modulating cycle in insolation. Now, our critical problem is to explain, physically and mathematically, the process through which equation (13) will modulate the insolation as a causal mechanism for climate change.

Physically, obliquity variation equations (1) and (2) represent an oscillaton signal whose

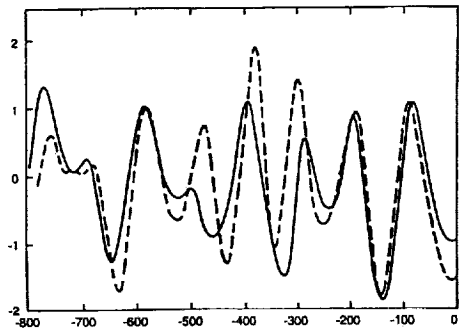

Figure 3. The solid curve denotes complex demodulation of the simulated temperature fluctuations caused by frequency variations in the obliquity. The dashed curve denotes complex demodulation of the $\delta^{18}O$ time series from [29].

amplitude is slowly varying with respect to frequency. Therefore application of obliquity variation as a component of insolation forcing for climate change should involve both the amplitude and frequency modulation, and their possible interactions or resonances. Frequency modulation is fully described by equations (4), (6) and (8). Since these frequency variation equations can be used to determine the lengthening/shortening of the cyclic period of the obliquity which are related to the prolonged glaciation and rapid melting of ice age ice sheets in the northern hemisphere, it seems justifiable to assume that climate model response to the incoming solar radiation is modulated by frequency variation of the obliquity.

Another question that might be asked is: Why should frequency modulation be considered as a forcing in climate models? We consider frequency modulation of the oblquity as a component of insolation forcing for climate change for the following reasons: (1) Its resonances with the insolation could induce pulses in the incoming solar radiation; climate response to these insolation pulses would cause major climate changes. (2) The lengthening/shortening of the cyclic periods of the obliquity, determined by equation (8), could be observed. (3) It can be recognized by performing modulation analysis on the complex demodulation of the geological data. (4) Finally, the frequency-insolation resonance effect seems to disappear before the mid-Pleistocene at about 900 kyr B.P. Our theoretical justification of the assumptions in the model is gratifying because it brings these important characteristics to light.

The motivation for equation (8) is the investigation of climate change via insolation. Ideally, equation (8) should provide (1) theoretical insights into the insolation and (2) a convenient formula for computing the insolation pulsation in the incoming solar radiation when using numerical climate models. The point of model simulation exercises is that equation (8) does seems to be suggestive of insolation modulation. Indeed, the test model indicates that equation (8) can be used to generate a 100-kyr modulating cycle in insolation. Therefore the simulation test of equation (8) as presented here is an example of the first motivation mentioned above. However, whether equation (8) fulfills the second motivation or not is yet to be established and justified.

The 100-kyr result of the model simulation test of equation (8) does not mean that it is a separate forcing function for climate change. The purpose of equation (8) is to provide a mathematical expression of physical reasons for modification of the insolation as a forcing function. It should be noted that there is a deep-seated misconception about the Milankovitch insolation forcing for climate change. According to phase theory, application of the Milankovitch insolation equation as a forcing function for climate change is

incomplete and inappropriate. Below it will be shown that frequency variation of the obliquity can induce insolation pulses and the pulse modulation of the insolation may provide an appropriate forcing mechanism to which the climate system would respond.

5. INSOLATION EQUATIONS

Milankovitch insolation function Q(t) is expressed in terms of orbital parameter variations.

$$Q(t) = \Delta R_s \Delta\varepsilon(t) + m\Delta(e\sin\omega) \quad (14)$$

in which ΔR_s is the difference of the insolation received at the top of the atmosphere over the caloric summer for 1^0 change in obliquity $\varepsilon(t)$, e sinω is the precession variation [2].

$$m = \frac{2T_y S\cos\phi}{\pi^2\left(1-e^2\right)^{1/2}} \quad (15)$$

where T_y is the duration of the tropical years, S is the solar constant, and ϕ is the latitude. Variations in orbital parameters (e, ε, esinω) are governed by

$$e = e_* + \sum_{i=1} E_i \cos\left(\lambda_i t + \zeta_i\right) \quad (16)$$

$$\Delta\varepsilon(t) = \sum_{i=1} A_i \cos\left(\gamma_i t + \xi_i\right) \quad (17)$$

$$\Delta(e\sin\omega) = \sum_{i=1} P_i \sin\left(\alpha_i t + \beta_i\right) - 0.0167\sin(102^*) \quad (18)$$

It is noted that equation (17) is the derivation from a constant of the obliquity $\varepsilon^\circ = 23.320556^\circ$ and equation (18) is the derivation from the present-day value of esinω. It is well known that orbital eccentricity *e*, obliquity change Δε(t) , and precession index Δ(esinω) oscillate at 100-Kyr, 41-Kyr and 23- or 19-Kyr, respectively. The peak-to-peak oscillation of the obliquity is about 2° [56].

New mathematical analysis to improve the accuracy of the constant in equations (16), (17) and (18) have been developed in [2, 41, 57-62]. ON the basis of these improved orbital constants, the time series from equation (14) for ϕ=65 *N* is shown in Figure 4 [22]. Its wavelet spectrum shows that the Milankovitch-type insolation forcing provides an almost negligible contribution from eccentricity forcing for the 100-kyr ice age cycles. A linear version of the Milankovitch insolation theory is inadequate to explain the 100-kyr glaciation cycle [3].

We propose to investigate how the climate system would respond to the amplitude-frequency resonance effect of the orbital parameters. In general, consideration of resonance in physics has proved to be enorously fruitful [63-69]. We argue here that it may provoke fundamental questions with regard to orbital forcing, insolation, and climate. In coming to grips with the physical meaning of the Milankovitch orbital forcing function, equation (14), as it relates to the nonlinear climate

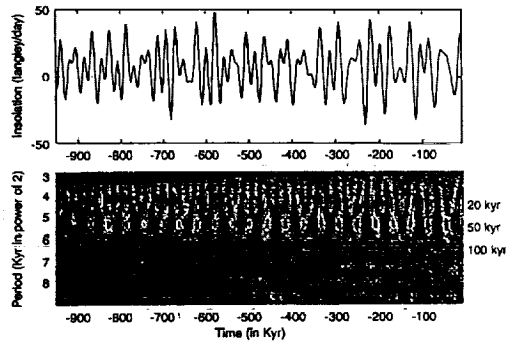

Figure 4. Milankovitch insolation at ϕ = 65°N and its wavelet spectrum.

problems, it is important to try to understand the concept of the instantaneous frequency of the insolation variations.

The instantaneous frequency hypothesis is that glacial and deglacial intensities are related to the frequency variations of the insolation. Ice ages started after the instantaneous frequency of the insolation reached minimum values, and deglaciations occurred at times when the instantaneous frequency of the insolation reached maximum values.

The time series from equation (14) is nonstationary and contains possible amplitude-frequency resonances in variations of the eccentricity, obliquity, and precession and their possible coupling interactions. Computing the instantaneous frequency of the insolation involves complex representation of the insolation function. The imaginary part of the function is actually the Hibert transform of the insolation Q(t) in equation (14). The Hibert transformation of insolation may provide a physical mechanism for climate change studies. However, we cannot make the Hibert transform for the Milankovitch insolation time series because the amplitude of the signal from equation (14) is not band-limited. It is possible that we can perform Hibert transform for the Rubincam insolation because the amplitude of the Rubincam insolation signal is in general band-limited.

To a high degree of approximation, the insolation F_s at any point on the Earth is given by [20]

$$F_S = F_S^{\cdot} H \cos\psi_S \left(\frac{r_{\cdot}}{r_S}\right)^2 \qquad (19)$$

where $F_s^0 = 1368\ Wm^{-2}$ is the average amount of sunlight impinging on the Earth, r_0 and r_s are the average and instantaneous distance from the center of the Earth to the center of the Sun respectively, Ψ_s is the solar zenith angel and $H=1$ when $\cos\Psi_s \geq 0$ and $H=0$ when $\cos\Psi_s < 0$. When $\cos\psi_s < 0$ the Sun is below the horizon and the flux is zero.

Rubincam [20] has developed equation (19) in terms of $(\varphi,\lambda,\eta,a,e,\varepsilon,\Omega,\omega,M)$ where φ is latitude, λ longitude, a the semimajor axis of the orbit, e the obliquity, Ω the nodal position, ω the argument of perihelion and M the mean anomaly, all these orbital parameters are referred to an Earth-fixed frame. The hour angle η, measured from a fixed point, describes the Earth's rotation.

In expressing insolation in terms of the Earth's orbital parameters, equations (19) becomes

$$\begin{aligned} F_S = F_S^{\cdot}\left(\frac{r_{\cdot}}{a}\right)^2 \sum_{l=0}^{\infty} d_l \sum_{m=0}^{l} (2-\delta_{0m}) \frac{(l-m)!}{(l+m)!} P_{lm}(\sin\varphi) \\ \cdot \sum_{p=0}^{l} \sum_{q=-\infty}^{\infty} F_{lmp}(\varepsilon) W_{l-2p,q}(e) \begin{bmatrix} \cos \\ \sin \end{bmatrix}_{l-m\,odd}^{l-m\,even} \\ \cdot \left[(l-2p)\varpi + (l-2p+q)M + m(\Omega-\eta-\lambda)\right] \end{aligned} \qquad (20)$$

which is the fundamental equation of insolation. In equation (20), the P_{lm} $(\sin\varphi)$ are the associated Legendre polynomials, F_{lmp} (ε) are the inclination functions commonly used in celestial mechanics, $W_{l-2p,q}(e)$ are eccentricity functions of the insolation and d_l are the coefficients of the insolation.

Averaging over the diurnal and annual cycles, leaves only the terms with $m = 0$ and $l-2p+q = 0$. Furthermore, $W_{n,-n} = 0$ for all $n > 0$, so that only $W_{0,0} = 1 + (1/2)e^2 + (3/8)e^4$ is non-zero. Finally, we note that d_l vanish for all odd l and decrease rapidly for all even l. Therefore, the truncation of $l > 2$ for equation (20) is a reasonable approximation for our

purpose. As a result, only the terms with $l = 0$, $p = 0$ and $l = 2$, $p = 1$, remain, and the zonal insolation to zero order in e is given by

$$F_S^{\phi}(t) = F_S^{\circ}\left(\frac{r_*}{a}\right)^2 \times \left\{\frac{1}{4} + \frac{5}{16} P_2(\sin\varphi)\left[\frac{3}{4}\sin^2\varepsilon(t) - \frac{1}{2}\right]\right\} \tag{21}$$

where $P_2(\sin\varphi)$ is the ordinary Legendre polynomial of degree 2, and terms in e^2 and e^4 are dropped due to their small values compared to 1. It should be noted that there is no $e \sin \omega$ terms in equation (21). Such terms depend on season, and the annual average is zero. But obliquity ε does appear. By writing $\varepsilon = \varepsilon(t) = \varepsilon^{\circ} + \Delta\varepsilon(t)$, dependence of the insolation on the obliquity $\Delta\varepsilon(t)$ becomes obvious. Combination of amplitude and frequency modulation of insolation may induce pulses in insolation.

6. PULSATION OF THE INSOLATION

Variations of the Rubincam insolation are computed from equations (17) and (21) for the past million years with an interval of 100 years. The results are shown in Figure 5. The real part of the complex vector of the insolation deviation $\Delta F_s^{\phi}(t) = F_s^{\phi}(t) - 222.125$ from equation (21) can be expressed by

$$\Delta F_S^{\phi}(t) = r(t)\cos[\theta(t)] = r(t)\cos[\varpi_c(t) + \zeta(t)] \tag{22}$$

where $r(t)$ is the amplitude, $\theta(t)$ is the argument, ϖ_c is the mean frequency of the insolation variations, and $\varsigma(t)$ is the phase angle. By convoluation theory [70, p.16] the imaginary part of insolation is defined by the Hibert transform

$$\langle \Delta F_S^{\phi}(t) \rangle = \frac{1}{\pi}\int_{-\infty}^{\infty} \frac{\Delta F_S^{\phi}(\tau)}{t-\tau} d\tau \tag{23}$$

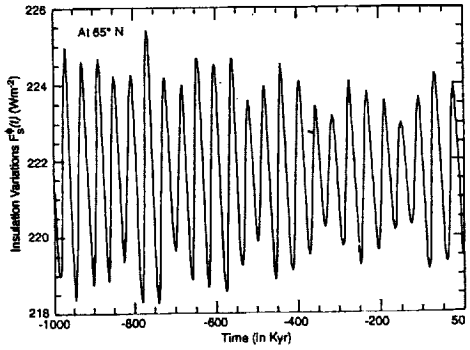

Figure 5. Variations in Rubincam's insolation.

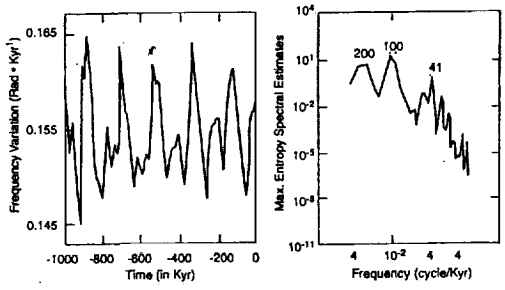

Figure 6. Frequency variations in Rubincam's insolation.

Therefore the time derivative of the phase angle ς is identical to the frequency variation of the insolation

$$\frac{d\zeta(t)}{dt} = \frac{d}{dt}\left\{\arctan\left[\frac{\langle \Delta F_S^{\phi}(t) \rangle}{\Delta F_S^{\phi}(t)}\right]\right\} - \varpi_c \tag{24}$$

The results of the phase modulation $d\varsigma(t) / dt$ of Rubincam's insolation and their spectrum are shown in Figure 6. Figure 6 shows that frequency of the insolation varies with 100-kyr and 200-kyr timescales.

Figure 6 may provide a physical

mechanism of the obliquity to cross the threshold of insolation. The threshold model presented here is actually derived from a signal-to-noise model. A threshold system [17,22,69,71] for insolation is shown in Figure 7. The insolation resonance consists of a threshold (shown by two horizontal dashed lines) and a subthreshold signal of the insolation at 65^0N (thin curve with its frequency modulation signal (thick curve). The addition of the frequency to the insolation curve (thin) enables Rubincam's insolation curve to cross the threshold. Each time the insolation intensity plus its corresponding frequency (normalized) increase across the threshold, a pulse (positive or negative) can be written to the time series. The quantized output is a pulse modulation train, which reproduces more closely the characteristics of the analog input signal (thick), indicating the insolation resonance of orbital forcing as a paradigm for mode (phase or period) locking [72] in the climate system.

To be more specific, the timing of insolation pulses essentially coincides with the occurrence of insolation resonances. These resonances with various magnitudes occurred at (-960, -910, -870, -800, -700, -630, -540, -500, -420, -330, -220, -130, -10) kyr and (-930, -820, -760, -650, -600, -470, -390, -270, -187, -70) kyr for rapid ice sheet melting and deep glaciation, respectively (Figure 7b).

The bipolar pulse modulation train *c(t)* in Figure 7b can be expressed by [70].

$$c(t) = \sum_i a_i P(t - t_i) - \sum_j a_j P(t - t_j) \quad (25)$$

where a_i and a_j are the magnitude of each unequally spaced pulse, and $P(t - t_i)$ and $P(t - t_j)$ are the basic pulse shape in which t_i and t_j are the time indices of insolation resonance.

The modulating function of the insolation

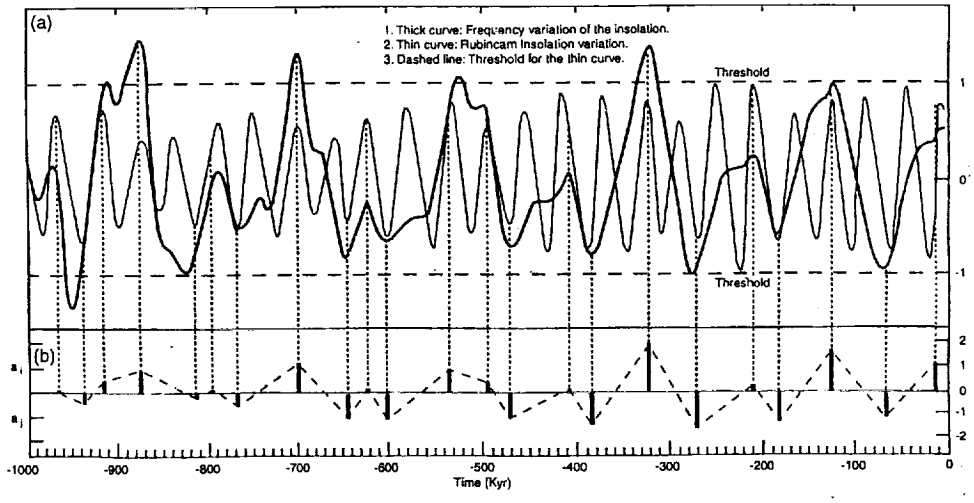

Figure 7. Obliquity variations cause resonances and pulses in insolation: (a) Amplitude-frequency resonances in insolation. (b) Bipolar pulse modulation train of the insolation. (a_i and a_j are the magnitude of each pulse)

signal $F_s^{\phi}(t)$ with a pulse modulation train $c(t)$ is $F_s^{\phi}(t)\,c(t)$. Therefore, from equations (17), (21), and (25) the structure of the pulse-modulated insolation can be expressed

$$\underline{P}\left[\Delta F_s^{\phi}(t)\right] = \Delta F_s^{\phi}(t)\left[1+\sum_i a_i P(t-t_i)-\sum_j a_j P(t-t_j)\right] \tag{26}$$

In trying to understand the behavior of insolation $F_s^{\phi}(t)$ as a forcing function for climate change the analytical formula obtained from orbital consideration can be applied using pulse modulation analysis. This is what has been shown in equation (26). The time series of equation (26) is nonstationary and contains a series of amplitude-frequency resonances due to the Earth's changing obliquity.

The interpretation of the nonlinear forcing function (equation 26) is that the pulse modulation is actually the combined effect of physical processes that is absent from the climate models: (1) negative insolation pulses that induce ice ages when insolation is reduced during downward cycles, at times when the frequencies are lower, and (2) positive insolation pulses that induce rapid ice sheet melting when insolation is increased during upward cycles, at times when frequencies are higher.

7. CLIMATE MODEL SIMULATIONS AND RESULTS

(a) Energy Balance Models

We have selected energy balance models to study the Baikal cycles and $\delta^{18}O$ variations because they are simple but realistic climate models. A class of zero-dimensional energy balance models (EBM) for climate change with surface temperature T as the main variable was developed by *Budyko [43], Sellers [44], Nicolis [45], North et al. [46],* and *Matteucci [5]* as one of the fundamental climate models. For a simplified version of EBM the equation of the model is

$$c\frac{dT}{dt} = \underline{P}\left[\Delta F_s^{\phi}(t)\right]\left[1-\alpha(T)\right]+E(T) \tag{27}$$

where c is the thermal capacity of Earth, $\underline{P}\,[\Delta F_s^{\phi}(t)]$ is the pulse-modulated insolation, $\alpha(T)$ is the globally averaged albedo, and $E(t)$ is the outgoing surface radiation as defined by equations (10) and (11).
Thus, from equations (26), (27), (10), and (11) we obtain

$$c\frac{dT}{dt} = \Delta F_s^{\phi}(t)\left[1+\sum_i a_i P(t-t_i)-\sum_j a_j P(t-t_j)\right] \cdot\left\{1-d_1+d_2\tanh\left[d_3(T-T_*)\right]\right\}-A-BT \tag{28}$$

The solution of equation (28) is a time series of T(t) as shown in Figure 8, superimposed on the time series of the biogenic

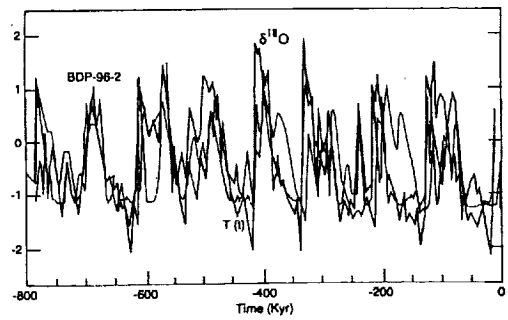

Figure 8. Calculated temperature variations T(t) compared to the marine $\delta^{18}O$ fluctuations and the continental biogenic silica cycles in Lake Baihal.

silica changes (Baikal Drilling Project (BDP)-96-2)) and $\delta^{18}O$ variations. The $T(t)$ curve indeed shows large variations of the same order of magnitude as seen in paleoclimate records [29, 30, 40]. To improve the accuracy of $T(t)$ in amplitude and phase, the global model should be extended to one-dimensional formulation.

For the 800 kyr time interval of overlap between the model results and proxy data, we have calculated their linear correlation and coefficients r. The Pearson coefficient r for the $T(t)$ - $\delta^{18}O$ and $T(t)$ - BDP correlation is about 0.85 and 0.87, respectively. These are significant enough to demonstrate their linear correlation. However, a simple statistical correlation with the marine and terrestrial paleoclimate records, although intriguing, is not a sufficient reason by itself to accept the hypothesis. To obtain a different view of the periodicity evolution, a wavelet spectrum analysis of the signals is needed [22]. We have performed wavelet spectral analysis of the time series of $T(t)$ and BDP and found that the characteristic spectral features in the $T(t)$ and BDP spectra are in good agreement with that of the $\delta^{18}O$ spectrum obtained by *Bolton et al.* [73], *Lau and Weng* [72], and *Liu and Chao* [22]. It is noted that coherency analysis of $T(t)$, $\delta^{18}O$, and BDP time series can also provide coherency spectra to understand their correlation in phase.

(b) Ice sheet Models

We have introduced the orbital resonance effect on insolation pulsation to examine the ice sheet climate models. The ice sheet climate models [19, 74-84] showed that the solar radiation variations due to orbital forcing are large enough to have produced ice ages. However, to make a small ice sheet grow to a critical large size or to make a critical large ice sheet decay rapidly, it is necessary that high rates of accumulation or ablation exist at least in the Northern Hemisphere during the glaciation and deglaciation phases. Therefore two predictions of ice sheet climate models should be tested against independent data: (1) higher rate of accumulation in the glaciation phase and (2) higher or rapid rate of ablation in the deglaciation phase.

Three parameters (a, b, and h_s) in Weertman's ice sheet model control the growth and decay of ice sheets: a is the accumulation rate, b is the ablation rate, and h_s is the elevation of the snow line. The half width L of an ice sheet can be formulated in terms of $a, b,$ and h_s. *Nye* [74, 75] and *Weertman* [76-78] showed that moderate changes in a, b, and h_s can change L by large amounts and can even make it impossible for such an ice sheet to exist. They have estimated that ~ 100 years of greater than normal accumulation or ablation caused by weather fluctuations would be long enough to induce a small ice sheet to start growing to a critical size or to melt a large ice sheet rapidly.

Under the low-low resonance conditions the negative insolation pulses last ~ 2 kyr longer than that in the normal glaciation cycles. Thus a small ice sheet would then expand into a critical large ice sheet as a result of increases in the accumulation rate for ~ 2 kyr. Rapid warming under high-high resonance conditions would increase the rate of change in $T(t)$ and hence increase the rate of ablation [84]. The maximum insolation during rapid deglaciation interval shifted ~ 2 kyr in advance. Therefore higher ablation rates would set in and persist for ~ 2 kyr longer than that in the normal deglaciation cycles. This seems to be the triggering mechanism for rapid melting of ice age ice sheets.

The center of the ice sheet on a continent in the Northern Hemisphere would shift southward as the ice sheet grows. The half width L of the ice sheet varies with time between the limits of about $0 < L < 1000$ km. On the northern edge of the ice sheet the snow line elevation is $h_{(x=-L)}(t)$, which varies in accordance with the variations in the ice sheet size. For reasonable variations in the values of a and b, Weertman's model showed that $h_{(x=-L)}(t)$ would fluctuate between the values of 0 and 0.6 km if variations in the half width L are limited to the range 0-1200km. Therefore the value of $h_{(x=-L)}(t)$ would be zero at the occurrence of the positive insolation pulsation and 0.6 km at the occurrence of the negative insolation pulsation. It is assumed in this simple way that the timing of the occurrence of the maximum and minimum values of the snow line elevation in the ice sheet is paced by the orbital resonance indices. Consequently, the elevation of snow line can be normalized and weighted by equation (26) [19].

The rate of change of the half width of ice sheet $dL(t)/dt$ is given by [78].

$$\frac{dL(t)}{dt} = \frac{2a}{3\beta^{1/2}}\{L(t) - \frac{(1+b/a)\beta}{4s^2} \cdot \left[\left(1+\frac{4sh_{(x=-L)}(t) - 2sL(t)}{\beta}\right)^{1/2} - 1\right]^2\}L^{1/2}(t) \quad (29)$$

in which s is the snow line slope of the ice sheet and $\beta = (4\tau)/(3\rho g)$, where τ is the basal shear stress, ρ is the density of ice, and g is the gravitational acceleration. Frequency modulated insolation (equation (26)) will undoubtedly cause changes in a, b, $h_{(x=-L)}(t)$ in equation (29), as discussed above. To include the nonlinear processes in the ice sheet climate model induced by the resonances in insolation, we have modified and weighted the ice sheet parameters (a, b, $h_{(x=-L)}$ (t) by equation (26), using the computation procedures developed by Liu [19]. Computer simulations were made incrementally by calculating $\Delta L(t)/\Delta t$, where Δt is taken as 1 kyr. The values of $\underline{P}[\Delta F_s^{\phi}(t)]$ were chosen for $\phi = 65°N$.

The results of computing equation (29) are shown in Figure 9. The time series of the half width of the ice sheet $L(t)$ from equation (29) seems to mimic the time series $\delta^{18}O$. Therefore introducing the frequency modulated insolation forcing function into the energy balance climate model and the ice sheet climate model yields reasonable matches to the observed climate records over the last 800 kyr (Figure 9).

We have applied the simple but realistic energy balance and ice sheet climate models to demonstrate the amplitude-frequency resonance effect of the insolation on climate change at high latitudes. However, these climate models were derived decades ago and the climate

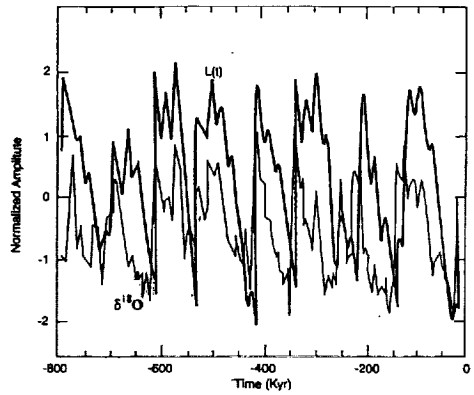

Figure 9. Calculated ice sheet variations L(t) compared to the marine $\delta^{18}O$ fluctuations from Ocean Drilling Project Site 677.

changes more or less than the global average, depending mostly on latitude. While changes of ~10°C would have occurred at high latitudes, changes of only ~2°C would have occurred near the tropical latitudes. In order to uncover the detailed latitudinal signiture of the proposed physical mechanism it is necessary to apply the full general circulation models of climate.

8. PHYSICAL MECHANISM OF OBLIQUITY FORCING

Although the results from model calculations show that equation (26) may provide a key element for the interpretation of the terrestrial and marine climate change, the physical mechanism by which the climate system is forced is still not clear. If the climate system instead reacts to the regular insolation forcing and responds primarily to the obliquity's phase variations, then a physical mechanism should be recognizable. For a physical mechanism to be considered appropriate and convincing, we will need to compute the obliquity-forced insolation variations in terms of energy flux at the top of the atmosphere.

When insolation is reduced during downward cycles of the obliquity, the total deficit of insolation on the top of the atmosphere in the Northern Hemisphere during a major (longer) glaciation period can be expressed by

$$\Delta E = \int_{t_1}^{t_2'} \Delta F_s^{\phi}(t)dt = k(\Delta E)_0 \qquad (30)$$

where t_1 and t_2' are the beginning and ending time of the longer glacial interval respectively. $\Delta F_s^{\phi}(t) = F_s^{\phi}(t) - 222.125$, k is a numerical factor, and $(\Delta E)_0$ is the average value of the total insolation deficit for a regular glacial interval. Computations of equation (30) for the past 10 major (longer) glacial time intervals yield $1.07 < k < 1.11$. Therefore, under resonance conditions the total insolation deficit on the top of the atmosphere during the longer glacial intervals is ~10% more than the average value $(\Delta E)_0$. This magnitude of insolation deficit seems sufficient to drive Earth into a deep ice age. Similarily, it can be shown that under resonance conditions the total insolation surplus on the top of the atmosphere in the Northern Hemisphere during the interglacial intervals is ~10% more than that of the regular deglacial intervals. The results of the insolation intergral over time (equation (30)) are illustrated as shown in Figure 10: under the low-low resonance conditions, the negative insolation pulse (area bfgb'b) provides a physical mechanism of insolation forcing for prolonged glaciation, and under the high-high resonance conditions, the positive insolation pulse (area dfed'd) provides a physical mechanism of the insolation forcing for rapid deglaciation. Figure 10 shows that both negative and positive insolation pulses last ~2 kyr. It should be noted that there are two types of pulsation: intensity pulsation and duration pulsation. The negative and positive pulses in Figure 10 are defined as duration pulsation, not intensity pulsation. It is the duration pulsation of insolation that drives the climate to oscillate with 100-kyr cycle.

Whatever the interpretation, the conclusion is that its realism can be measured by calculating the integral of equation (30) over time for having only an obliquity signal. This kind of insolation calculation can be used in the EBM to scale the resonance effect in insolation on climate change.

Indeed, ignoring the pulsed source of insolation, $F_s^{\phi}(t)$ forces the model to give 0.4°C

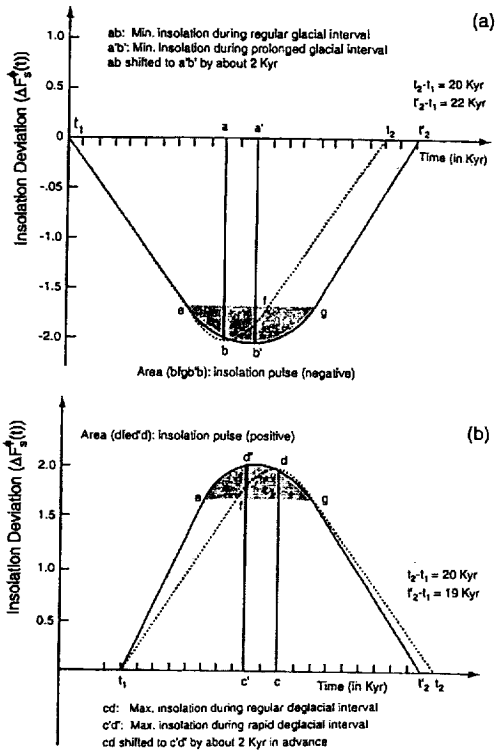

Figure 10. Physical mechanism of insolation forcing for climate change for (a) low-low resonance conditions and (b) high-high resonance conditions.

for the temperature range, which is in agreement with the results obtained by *Matteucci* [5]. However, modified by insolation pulses due to insolation resonances, equation (26) forces the model to give ~10^{0}C for the temperature range. This shows that the magnitude and the formulation of the phase modulation influence of Rubincam's insolation for climate change are too big and important to be dismissed, even at a preliminary stage.

As a forcing function, equation (26) shows that the climate system should respond not only to variations in the time-dependent insolation but also to a combined effect of changes in insolation and frequency of its quasi-sinusoidal variation. This is quite different from arguing that the system is highly nonlinear and threshold driven. From climatologist's point of view, interpretation of the forcing function is that the pulse modulation introduced here is actually a physical property of orbital dynamics that is absent from the climate models.

9. WAVELET SPECTRUM OF THE MODELED TEMPERATURE VARIATIONS

For the 800 kyr time interval of overlap between the model results and proxy data, we have calculated the Pearson's linear correlation coefficient r between the signals. The value of the Pearson's r is about 0.85, which is significant to support our conclusions. However, a simple statistical correlation with the paleoclimate record is not a sufficient reason by itself. For a new view of the periodicity evolution, a wavelet spectrum analysis of the signals is needed. [22].

Nonstational cycles abound in the time series $T(t)$ from equation (28). The time-frequency spectral behavior of this model output data is of theoretical and practical interest. The most important feature of the $T(t)$ time series is that its 100-kyr cycle is not stable through time.

Advanced spectral tools such as Blackmann-Tukey, maximum entropy, and highly efficient Thomson technique have been applied to investigate the paleoclimatic variability using a set of four deep core data [85]. The dominant feature is the presence of a

period centered at 117 kyr. One of the best paleoclimate records is the $\delta^{18}O$ curve, obtained by *Shackleton et al.* [29]. Recently, *Bolton et al.* [73] and *Lau and Weng* [72] have performed wavelet spectral analysis on the $\delta^{18}O$ time series and found that the 100-kyr cycle in the wavelet spectrum of the $\delta^{18}O$ data is time dependent. In this regard, we have performed wavelet spectral analysis on the $T(t)$ time series to demonstrate that this model for Pleistocene climate provides a good fit to the time evolution characteristics in the wavelet spectrum of the observed $\delta^{18}O$ data.

The wavelet transform of the time series $T(t)$ with respect to the analyzing wavelet $g_{(a,b)}(t)$ can be defined as a convolution integral [86]

$$Wg_{(a,b)}(t) = a^{-1/2}\int_{-\infty} T(t)g^{*}\left(\frac{t-b}{a}\right)dt \qquad (31)$$

where a denotes the scale (dilation), b denotes the position (translation) and $g^{0}[(t - b)/a]$ is the complex conjugate of $g_{(a,b)}(t)$ defined on the open real (a, b) half plane. The wavelet spectrum is thus displayed in the time-frequency domain, or the a-b space with the horizontal time axis b and the vertical frequency axis a. For our application we select the Morlet wavelet [87] which is a normalized, Gaussian-enveloped complex sinusoid with zero mean. We choose to examine the real part of the wavelet transform. It gives the amplitude undulation with the appropriate polarity and phase with respect to time owing to the symmetric nature of the real part of the Morlet wavelet as the kernel in integral equation (31). In contrast, the imaginary part, being antisymmetric in the kernel, gives the amplitude undulation as well, but imparts a 90^{0} phase shift in time. In many application cases the modulus (combining real and imaginary parts) is preferred, but then the polarity phase information, which is important in our study, becomes absent. We use color contours such that amplitude peaks and troughs in horizontal successions in high contrast colors indicate the presence of strong oscillations in the data, relative to the weaker and less significant background of low color contrast [22].

A wavelet spectrum of the time series $T(t)$ thus developed is shown in Figure 11. One of the most important spectral features in Figure 11 is that the 100-kyr cycle is not stable through time. After -650 kyr a near 100-kyr cycle dominates the spectrum, reflecting stronger pulses in the modulated radiation deviation. Prior to this time, in the region of time-frequency space near -850 kyr to -650 kyr, a near 80-kyr cycle emerges, in addition to a weakened 120-kyr cycle. Obviously, this is attributable to the strength and timing of the amplitude-frequency resonances of the obliquity. In this way, pulse modulation of the incoming solar radiation due to the amplitude-frequency resonance of the obliquity may cause the 100-kyr climate cycle.

Indeed, the model results show a transition from dominant 41-kyr to dominant 100-kyr period about 900 kyr ago, as seen in the paleoclimatic record. Therefore the wavelet spectrum of the model's results (Figure 11) explains clearly the periodicity evolution of the paleoclimatic fluctuations over the past 2 million years. A simple Fourier analysis would suffice to prove that the paleoclimatic record is nonstationary over the whole Pleistocene. However, it can not demonstrate its periodicity evolution.

The time-frequency spectral behavior of the model output as shown in Figure 11 is in good agreement with that of the $\delta^{18}O$ record

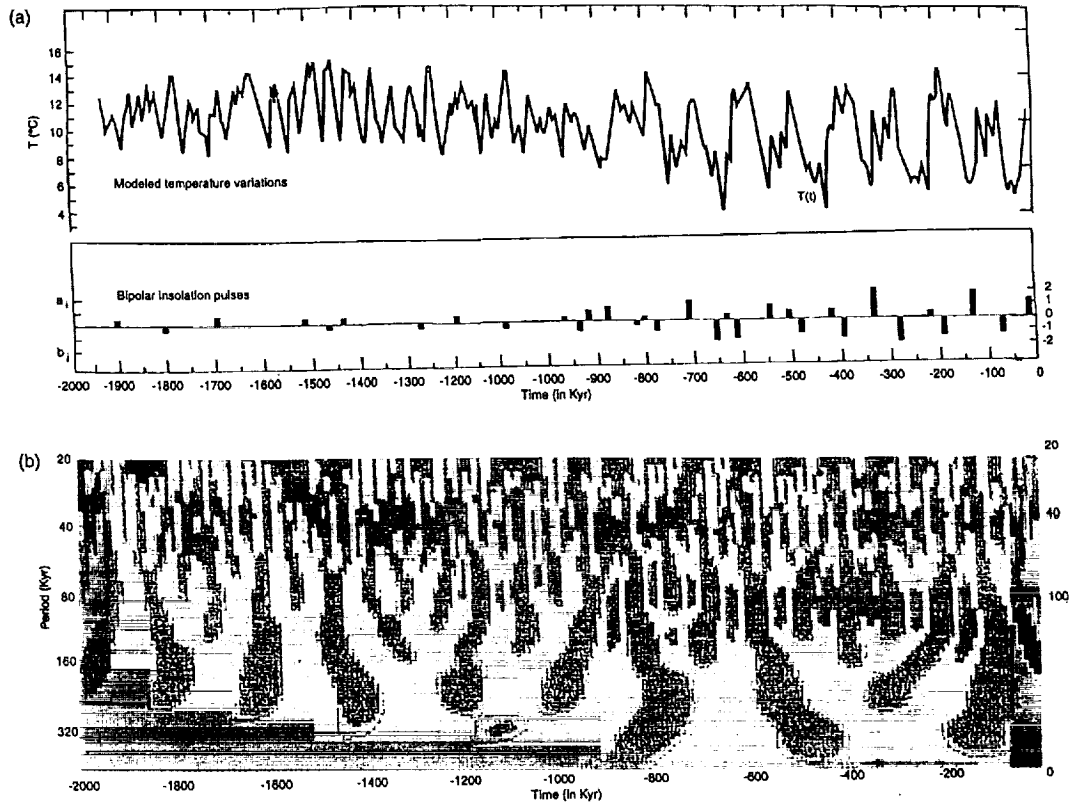

Figure 11. (a) Temperature variations and bipolar insolation pulses from the model and (b) wavelet spectrum of the temperature variations for the past 2 million years.

[72,73]. We note that since the publication of the paper by *Hays et al.* [88], numerous modeling efforts have attempted to explain the relation between Milankovitch insolation forcing and climate change. Most of these modeling studies have focused on the origin of the 100-kyr cycle. What these models do confirm is that climate response to Milankovitch forcing is nonlinear and that it involves some elements of internal forcing. However, whether the Milankovitch external orbital forcing drives the internal forcing [3], phase locks the oscillations of an internally driven system [89], or acts as pacemaker for the free oscillations of an internally driven system [90] is an open question. Furthermore, internal forcing mechanisms or feedbacks have difficulties in explaining the apparently episodic appearance of the 100-kyr cycle [40]. It remains to be seen if the wavelet spectra of the output data from climate models with internal forcing can fit the spectral of the $\delta^{18}O$ record

[72,73].

10. PHYSICS BEHIND ICE AGE GLACIATION

The physics behind the marine and continental ice age glaciations can be explained as follows. The insolation forcing mechanism which is capable of reproducing of ice age ice sheet is illustrated in Figure 10, in which the insolation flux deficit *(bfgb'b)* is the physics behind the ice age glaciation. The areas *ebfe* and *eb'ge* represent the regular and prolonged glaciation phases respectively; their area ratio is about 1:2. It also shows that the minimum insolation *a b* during regular glacial phase shifted about 2 Kyr to the minimum insolation *a'b'* during the prolonged glacial phase. While the regular glaciation phase lasts only about 4 Kyr, the prolonged glacial phase lasts longer than 8 Kyr. Physically, ice sheet size would grow larger if glaciation time is longer and glacial phase becomes broader. Therefore, we have reason to believe that the negative insolation pulse *bfgb'b* is responsible for the 100-Kyr cycle of ice age glaciation. Here, we identify the insolation flux deficit *bfgb'b* in Figure 10 as the causal mechanism responsible for the amplification of an external forcing by the orbital resonance dynamics, and arrived in this way at a better understanding of the role of an externally generated factor in climate change. This causal mechanism is appropriate and convincing because: 1. The timing of the *bfgb'b* occurrence coincides with the observed major climate change events; and 2. The insolation flux deficit represented by *bfgb'b* is powerful enough to drive the Earth into an ice age.

The determination of continental temperature variations in Siberia by Williams et. al. [30] lends fresh support to the theory that frequency variation of the obliquity is the main mechanism responsible for the late Pleistocene climate change. Because Lake Baikal is located in the continental interior, its biological productivity is sensitive to solar energy variations, which are accurately recorded through the flux of biogenic silica to the bottom sediments.

The model time series *T(t)* is shown in Fig. 8, superimposed on the time series of the oxygen isotope content $(\delta^{18}0)$ of deep-sea sediments and the biogenic silica changes (BDP-96-2) of the terrestrial sediments from the Baikal Drilling Project (BDP). The *T(t)* curve indeed shows variations of the same order of magnitude and phase as seen in the paleoclimate records [29, 30, 40]. This implies that the marine and the continental 100-Kyr ice age cycles are driven by a simple orbital mechanism: frequency modulation of the obliquity.

The canonical view of the marine oxygen isotope fluctuations is that they are attributed to the internal feedback mechanisms in the ocean-atmosphere-cryosphere system that can change atmosphere temperatures, CO_2, methane, ice sheets, ocean circulation and sea surface temperatures [3]. If this view were correct, then the far more perplexing mystery may be how to explain the continental 100-Kyr ice age cycles. Because the continental biological productivity is independent of ice sheet size, changes in ocean circulation or atmosphere CO_2 concentration, the physical mechanisms of internal forcing for continental climate change are far from obvious. The continental 100-Kyr puzzle may prove even more mysterious than the marine 100-Kyr puzzle [30].

11. INTERPRETATION OF GLACIATION PUZZLES

Pulsation of insolation induced by the

frequency variations of the Earth's obliquity may provide explanations for the 3 glaciation puzzles in paleoclimatology.

The first puzzle in paleoclimatology has been understanding why the major glaciation cycles of the last 1 million years vary at a 100-Kyr rhythm. Although the Earth's orbital eccentricity has a 100-Kyr cyclicity, the resulting changes in insolation are too small to be climatically significant. The second puzzle is how to explain the first two million years of the northern hemisphere ice ages when global ice volume and ocean temperature varied predominantly at the 41-Kyr period of the Earth's obliquity. The variation in summer insolation at high latitudes is dominated by precession. If the Milankovitch view that summer radiation at high latitudes exerts the ultimate control on ice sheet mass balance is correct, then far more precessional variance at 23-and 19-Kyr would be observed in high latitude climate records of the late Pliocene and early Pleistocene. Lastly, we still don't understand why the 100-Kyr cycle became abruptly dominant about 900 Kyr ago. In the past decade, numerous hypotheses have been proposed to explain these puzzles; however, every explanation has had difficulty accounting for the causal mechanisms of orbital or stochastical forcing for climate change [3-7, 10, 11, 13, 14, 16, 17, 91-93]. From a climatologist's point of view, the physical mechanism of climate change and the rules that govern climate transitions between states involve ocean-atmosphere-ice processes on time scales that are paced by orbital variations. Therefore, it is generally believed that only through the continued collection and analysis of geological data from deep ocean drilling and continental drilling can we hope to come to a deeper understanding of the mechanisms by which the global climate system responds. On the contrary, we have shown here that our understanding of the dynamics of orbital forcing for climate change is far from complete. We still have huge gaps in our understanding of the first-order orbital resonance effect on climate change, gaps which can only be filled by fundamental physics. Based on orbital resonance theory, this study demonstrates that the orbital parameter which paces for the 100-Kyr ice age cycle is actually the frequency variation of the Earth's obliquity, not orbital eccentricity. As shown in Figure 11, temperature varies for the past 2 million years predomintly at the 41-Kyr period of the obliquity. Also, the modeled 100-Kyr temperature variation as shown in Figure 11 becomes dominant abruptly about 900 Kyr ago. Why did the 100-Kyr cycle only appear about 0.9 million years ago? Because since that time cooperative phenomena between the frequency and amplitude variations of the obliquity have induced a resonance effect on climate response to insolation, so as to shift the 41-Kyr cycle into the 100-Kyr cycle.

12. CONCLUDING REMARKS

The study of how frequency variation of the Earth's obliquity came to be related with the paleoclimatic changes has recently moved into a new phase of scientific inquiry and discovery. Notable advances in atmospheric science have given rise to new ways of insolation calculation to solve the perplexing and enduring glaciation puzzles in paleoclimatology. The focus of this review is on the problem in insolation theory of climate change. The problem is that all ice models were introduced in the climate system without the appropriate time-dependent response to the energetics of the climate system. In order to make up for this deficiency in the climate system, we have introduced a pulsation term of insolation as a device for illustrating the physics behind the glacial cycles.

This has been done in terms of a bipolar pulse modulation train $c(t)$ of insolation. According to theories of resonance, insolation pulsation has been applied to characterize the time-dependent response of ice models in the climate system. Incorporating the amplitude-frequency resonance effect of the obliquity, climate model simulations have delivered an ice age chronology that is in close accord with $\delta^{18}O$ and BDP proxy data. This methodology of insolation pulsation is developed from a convolution theory of the non-stationary time series of insolation by the Hibert transformation in order to find out the three glaciation puzzles in paleoclimatology. The success of the model simulation results is remarkable because they can provide explanations to account for the origin, structure and spectrum of the observed major climate changes during the past 2 million years. In conclusion, we claim that frequency modulation effect of the Earth's obliquity on the incoming solar radiation may be the key to solving the century-long glaciation puzzles in climatology.

ACKNOWLEDGMENTS

Computations were performed by Clarence Wade Jr. at the Laboratory for Astronomy and Solar Physics. The author thanks Albert Arking, Bruce G. Bills, Benjamin F. Chao, Linda A. Hinnove, Derek L. Ho, David P. Rubincam and Hengyi Weng for discussions.

REFERENCES

1. Milankovitch, M. 1930, Handbuch der Klimatologe, Borntrager, Berlin.
2. Vernekar, A. D. 1972, Meterol. Monogr., 12, 1.
3. Imbrie, J., and 18 co-authors 1993, Paleoceanography, 8, 699.
4. Rial, J. A. 1995, Geophys. Res. Lett., 22, 1997.
5. Matteucci, G. 1987, Clim. Dyn., 3, 179.
6. Saltzman, B., and Verbitsky, M. 1994, Paleoceanography, 9, 767.
7. Pollard, D. A. 1982, Nature, 296, 334.
8. Hyde, W.T., and Peltier, W. R. 1985, J. Atmos. Sci., 42, 2170.
9. Imbrie, J., and 17 co-authors 1992, Paleoceanography, 7, 701.
10. Raymo, M. E. 1997, Paleoceanography, 12, 577.
11. Raymo, M.E. 1998, Science, 281, 1467.
12. Tarasov, L., and Peltier, W. R. 1997, J. Geophys. Res., 102, D18, 21665.
13. Berger, A., Li, X.S., and Loutre, M. F. 1999, Quat. Sci. Res., 18, 1.
14. Muller, R. A., and MacDonald, G. J. 1995, Nature, 377, 6545, 107.
15. Muller, R. A., and MacDonald, G. J. 1997a, Science, 277, 5323, 215.
16. Muller, R. A., and MacDonald, G. J. 1997b, Proc. Nat. Acad. Sci. U.S.A., 94, 16, 8329.
17. Paillard, D. 1998, Nature, 391, 378.
18. Liu, H. S., 1992, Nature, 358, 397.
19. Liu, H. S., 1995, Earth Planet. Sci. Lett., 131, 17.
20. Rubincam, D. P. 1994, Theor. Appl. Climatol., 48, 195.
21. Rubincam, D. P. 1996, Theor. Appl. Climatol. 53, 257.
22. Liu, H. S., and Chao, B. F. 1998, J. Atmos. Sci., 55, 2, 227.
23. Liu, H. S., 1998a, Theor. Appl. Climatol., 61, 217.
24. Liu, H. S., 1998b, J. Geophys. Res. (Atmos.) 103, 26147.
25. Liu, H. S., 1999, J. Geophys. Res., 104, 25197.
26. Broecker, W. S., and Van Donk, J. 1970, Rev. Geophys., 8, 168.
27. Prell, W. L., and 6 co-authors 1986,

Paleoceanography, 1, 137.
28.Sarnthein, M., and Tiedmann, R. 1990, Paleoceanography, 5, 1041.
29.Shackleton, N. J., Berger, A. and Peltier, W. R. 1990, Tran. R. Soc. Edinburgh Earth Sci. Rev., 81, 251.
30.Williams, D. F., and 6 co-authors 1997, Science, 278, 1114.
31.LeVerrier, U. 1855, Ann. Observ. Imp. Paris, II, 43.
32.Croll, J. 1867, Philos. Mag., 33, 426.
33.Berger, A., and Loutre, M.F. 1990, Bull. Cl. Sci. Commun. Acad. R. Belg., Paleoclimatol., Ser. 6, 45.
34.Kinoshita, H. 1977, Celestial Mech., 15, 277.
35.Brouwer, D. and Clemence, G. M. 1961, Methods of Celestial Mechanics, Academic Press, New York.
36.Brouwer, D., and van Woerkom, V. 1950, Astron. Pap. Am. Ephemeries, 13, 83.
37.Broecker, W. S. 1992, Nature, 359, 779.
38.Ludwig, K. R., and 6 co-authors 1992, Science 258, 284.
39.Winograd, I. J., and 7 co-authors 1992, Science, 258, 255.
40.Beaufort, L. 1994, Paleoceanography, 9, 821.
41.Laskar, J. 1988, Astron. Astrophys., 198, 341.
42.Berger, A., and Loutre, M. F. 1991, Quat. Sci. Res., 10, 297.
43.Budyko, M.L. 1969, Tellus, 21, 611.
44.Sellers, W.D. 1969, J. Appl. Meteorol., 8, 392.
45.Nicolis, C. 1980, J. Geophys. Astrophys. Fluid Dyn., 14, 91.
46.North, G. R., Cahalan, R. F. and Coakley, J. R. 1981, Rev. Geophys., 19, 91.
47.Bhattacharya, K., Ghil, M., and Vulis, I.L. 1982, J. Atmos. Sci., 38, 1747.
48.Jouzel, J. C., and 6 co-authors 1987, Nature, 329, 403.
49.Genthon, C.J., and 7 co-authors 1987, Nature, 329, 414.
50.Broecker, W. S., and Denton, G. H. 1989, Geochim. Cosmochim. Acta, 53, 2465.
51.Grootes, P. M., and 4 co-authors 1993, Nature, 366, 552.
52.Johson, S., and 9 co-authors 1992, Nature, 359, 311.
53.Cuffey, K. M., and 5 co-authors 1995, Science, 270, 455.
54.Bloomfield, P. 1976, Analysis of Time Series, John Wiley, New York.
55.Shackleton, N. J., T. K., and Crowhurst, S. J. 1995, Paleoceanography, 10, 693.
56.Chao, B. F. 1996, EOS, Trans. Am. Geophys. Union, 77, 433.
57.Berger, A. 1976, Astron. Astrophy.,51, 127.
58.Berger, A. 1977, Nature, 268, 44.
59.Berger, A. 1988, Rev. Geophys., 26, 624.
60.Quinn, T. R., Tremaine, S., and Duncan, M. 1991, Astron. J., 101, 2287.
61.Richardson, D. L., and Walker, C. F. 1989, J. Astron. Sci., 37, 159.
62.Williams, J. G., Newhall, X. X. and Dickey, J.O.. 1991, Astron. Astrophys., 241, 9.
63.Liu, H. S. and O'Keefe, J.A. 1965, Science, 150, 1717.
64.Laslett, L. J., and Sessler, A. M. 1966, Science, 151, 1384.
65.Jeffreys, W. H. 1966, Sciences, 152, 201.
66.Monteoliva, D. B., Borsch, H. J. and Nunez, J. A. 1994, J. Phys. A. Math. Gen., 27, 6897.
67.Sutera, A. 1981, J. Atmos. Sci., 37, 245.
68.Gammaitoni, L. 1995, Phys. Rev. E, 52, 4691.
69.Bulsara, A. R., and Gammaitoni, L. 1996, Phys. Today, 3, 39.
70.Rowe, H.E. 1965, Signal and Noise in Communication Systems, Van Nostrand Reinhold, New York.
71.Wiesenfelt, K., and Moss, F. 1995, Nature, 373, 33.
72.Lau, K-M, and Weng, H. 1995, Bull, Am. Meteor. Soc., 76, 2391.

73.Bolton, E. W., Maasch, K. A., and Lilly, J. M. 1995, Geophys. Res. Lett., 22, 2753.
74.Nye, J. F. 1959, J. Glaciol., 3, 493
75.Nye, J. F. 1960, Proc. R. Soc. London, Ser. A, 256, 559.
76.Weertman, J. 1961, J. Geophys. Res., 66, 3783.
77.Weertman, J. 1964, J. Glaciol., 5, 145.
78.Weertman, J. 1976, Nature, 261, 17.
79.Birchfield, G. E., and Ghil, M. 1993, J. Geophys. Res., 98, 10385.
80.Pollard, D. A. 1982, Nature, 296, 334.
81.Watts, R.G., and Hayder, M.E. 1961, J. Geophys. Res., 66, 3783.
82.Peltier, W. R. 1982, Adv. Geophys., 24, 2.
83.Ghil, M. 1984, J. Geophys. Res., 89, 1280.
84.Oerlemans, J. 1994, Science, 264, 243.
85.Berger, A., Melice, J. L., and Hinnov, L. 1991, Clim. Dyn., 5, 227.
86.Erlebacher, G., Hussaini, M.Y., and Jamson, L. M. 1996, Wavelet: Theory and Applications, Oxford Univ. Press, New York.
87.Morlet, J., Arehs, G., Fourgean, I. And Giard, D. 1982, Geophysics, 47, 203.
88.Hays, J. D., Imbrie, J., Shackleton, N. J. 1976, Science, 194, 1121.
89.LeTrout, H., Portes, J., Jouzel, J., and Ghil, M. 1988, J. Geophys. Res., 93, 9365.
90.Maasch, K. A., and Saltzman, B. 1990, J. Geophys. Res., 95, 1955.
91.Short, D. A., and 4 co-authors 1991, Quat. Res., 35, 157.
92.Rial, J. A. 1999, Science 285, 564.
93.Willis, K. J., Kleczkowski, A., Briggs, K. M., and Gilligan, C. A. 1999, Science, 285, 568.

POPULAR SUMMARY

Astonomical Background:

* Frequency modulation of the Earth's obliqity is the major cause of climate change. It was misleading to call upon other astronomical forcing such as orbital eccentricity, inclination and precession to explain the origin of the ice-age cycle which is a mystery in science.

Geophysical Speculations:

* The varying frequency of the obliquity can induce pulses in the incoming solar radiation. Glacial and interglacial climate events are the consequence of insolation pulsation. It is unnecessay to speculate internal feedbakes such as ocean circulations and atmospheric CO_2 concentrations in the Earth system to understand the glaciation puzzles.

Geological Data:

* Results from model simulations are in good agreement with geological climate records for the past 2 million years.

Climate Prediction:

* Extension of model simulation reveals that the current warming trend of the climate is almost over and will give way to forecast a small ice age.